

## Numerical model of the selectivity effect and the $\Delta V/L$ criterion

N. Sarlis, M. Lazaridou, P. Kaporis, and P. Varotsos

Solid Earth Physics Institute, Physics Department, University of Athens

**Abstract.** Numerical solutions of Maxwell equations for a model earth with a reasonably conducting channel indicate that the electric field values are intensified within a certain region *only* (i.e., above the end of the channel), thus explaining the observed *selectivity effect*. In this region, the electric field may reach detectable values (5-10mV/km), while the magnetic field still remains low ( $10^{-2}$ nT). The results are compatible with those obtained recently by analytical solutions (Varotsos *et al.* [1998]). Both the numerical and the analytical solutions lead to a natural explanation of the  $\Delta V/L \approx \text{const}$  criterion. This criterion, however, should not be applied over an area with strongly inhomogeneous electrical structure.

### Introduction.

The SES observations revealed the so called *selectivity effect*, e.g., Varotsos and Lazaridou [1991], Varotsos *et al.* [1993,1996a], Uyeda [1996], which consists of two facts: (i) SESs are observed at particular sites of the earth's surface ("sensitive sites") and (ii) each "sensitive site" can record SESs from certain focal areas. Varotsos *et al.* [1998] recently published analytical solutions showing that the selectivity effect is a direct consequence of Maxwell equations, if we consider that the earthquake (EQ) preparation zone lies in the vicinity of a fault, which provides an example of a conductive path for the transmission of the electric signal. These solutions indicate that there are two regions on the earth's surface that are sensitive for SES collection: one region is just above the EQ source when its depth is not large, and the other is around the upper end of the conductive path. In the present paper we show that numerical solutions of Maxwell equations lead to similar conclusions.

### The model.

Varotsos and Alexopoulos [1986] and Varotsos *et al.* [1993] suggested the following model for the SES transmission. When the SES is emitted, the current follows the most conductive channel through which most of this current travels; if the emitting source lies near a channel of high conductivity (Fig. 1) and the measuring station lies at a site (see the point "O") close to the upper end of the conductive channel, the electric field is appreciably stronger than in the case of a homogeneous or horizontally layered earth.

As we are mainly interested in the case where the focal depth is within the range of 5-50 km, we can safely assume that the "host rock" has a resistivity  $\rho_0$  between  $10^3 \Omega\text{m}$  and  $10^4 \Omega\text{m}$ . As a first approximation, we select the value  $\rho_0 \approx 4 \times 10^3 \Omega\text{m}$  (Varotsos *et al.* [1998]). The surface layer with depth  $\sim 50\text{m}$  may have a typical resistivity value  $\rho_s \approx 200 \Omega\text{m}$ . The resistivity  $\rho_f$  of a fault is known to be around  $10 \Omega\text{m}$ , giving the conductivity  $\sigma_c$

of the channel,  $\sigma_c = (1/\rho_f) = 0.1 \Omega^{-1}\text{m}^{-1}$  (Varotsos *et al.* [1996b]). Concerning the width  $w$  of the channel, we may assume values of the order of 100 to 1000m, but we shall make the calculation with a mean value of  $w \approx 500\text{m}$ . The same value of 500m was assumed for the thickness and hence the conductance  $\tau$  is  $0.1 \times 500 = 50\text{S}$ . The current dipole is assumed, for simplicity, to be oriented along x-axis (cf. cases for other orientations have been described elsewhere [Varotsos *et al.* 1999a]) and its projection on the earth's surface lies at a distance of 100km from the point (0,0,0) which represents the projection on the earth surface of the channel's upper end (Fig. 1).

In summary, our problem involves a two layer earth (with a 50m surface layer with resistivity  $\rho_s = 200 \Omega\text{m}$ , and a host with resistivity  $\rho_0 = 4000 \Omega\text{m}$ ) and a conductive channel with resistivity  $\rho_c = 10 \Omega\text{m}$ , which is buried at outcrop depth  $h = 100\text{m}$  and directed downwards so that it has a depth of 5km at 100km from its outcrop. The dimensions of the channel were taken either  $500\text{m} \times 500\text{m} \times 100\text{km}$  or  $500\text{m} \times 500\text{m} \times 200\text{km}$  and it was modelled by a thin sheet of conductance  $\tau = 50\text{S}$  (depicted in the insets of Fig. 1A and 1B). We clarify that, within the constraint of the thin sheet approximation, the situation should be modelled by an almost horizontal thin-sheet rather than a vertical one when aiming at determining the spatial distribution of the electric field on the earth's surface.

The results were obtained in the frequency range of  $10^{-2}$  Hz by running the EMIDSH program (the details and the calculation scheme can be found in Hoversten and Becker [1995]), with two different rectangular grids of  $6 \times 150$  and  $5 \times 200$  cells. Only the field values that have less than 20% discrepancy between the two discretizations were used for the further analysis, and the respective errorbars in diagrams depict the extent of this discrepancy. The real problem was modelled by a scale  $L_m = 10^{-7} L_w$  following the "similitude relationship" that relates the frequency  $\omega$ , magnetic permeability  $\mu$ , conductivity  $\sigma$ , and length scale  $L$  of a real world problem to a model problem:  $\omega_m \mu_m \sigma_m L_m^2 = \omega_w \mu_w \sigma_w L_w^2$ , where the subscripts w and m denote the real world and the model problem parameters. (The current source was scaled, of course, by the corresponding factor  $10^{-7}$ .)

### Results.

Figures 2A-2C are the results of the calculation for the case of Fig. 2D; the distribution of the amplitude of the horizontal component  $E_x$  of the electric field on the XZ plane,  $Y=0$  and on the XY plane,  $Z=0$  i.e., at the earth's surface, is shown in Figs 2A and 2B respectively, while Fig. 2C depicts  $E_y$  at the earth's surface. All the values have been reduced by the magnitude  $E_{\text{host}}(-100,0,0)$  of the electric field that would be measured just above the source on the earth's surface in the absence of the channel. Figure 2B indicates that there are two regions on the earth's surface in which  $E_x$  may be detectable provided that the source dipole is strong enough to give there  $E_x$  values exceeding the noise level: one region lies close to the channel's upper end and another one just above the source. Repeating the calculation for larger depths of the source, e.g.,  $z=50\text{km}$ , and comparing the values in these two regions (see Fig. 3), we find that the electric

Copyright 1999 by the American Geophysical Union.

Paper number 1998GL005265.

0094-8276/99/1998GL005265\$05.00

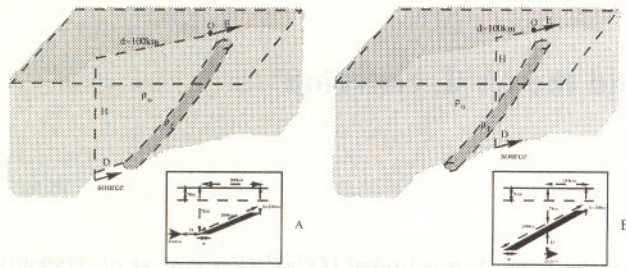


Figure 1. Schematic representation of SES transmission models.

signals may become stronger close to the channel's upper end than directly above the source when the source becomes deeper, thus explaining the signal detection at larger epicentral distances, but not at shorter. (cf. The "anomaly" in Fig. 3, i.e., the abrupt decrease and then increase of  $E_x$ , simply reflects the fact that  $E_x$  changes sign -passing through zero- while the magnitude of the total electric field remains finite).

Note that the results above have been obtained for the case of the model of Fig. 1B. The values of  $E_x$  above the channel's upper end only slightly depend on the width  $w$  (in the range  $w=500-1000\text{m}$ , see Fig. 3) as well as on the vertical distance  $D$  of the source from the channel (see the open circles in Fig. 4), thus agreeing with the earlier conclusions of *Varotsos et al.* [1998]. If we repeat the calculation for the case of the model depicted in Fig. 1A we find the solid dots in Fig. 4 which show that at small horizontal distance  $D$  the electric field values are very large. The latter is compatible with analytical solutions (see the Appendix) and its physical significance as well as the influence of the width will be discussed, in detail, elsewhere (*Varotsos et al.* [1999a]).

We now turn to the magnetic field values (B) which are also calculated by the program. In the case of the aforementioned model of Fig.2D, we find that, for dipole sources of the order of  $10^6\text{Am}$  (which, as explained by *Varotsos et al.* [1998], might correspond to  $M\sim 5$ , if we assume solid state generation mechanisms), and for the region above the upper end of the channel, the electric field values are  $5-10\text{mV/km}$  (see Fig.4) while the calculated B-values are  $\sim 10^{-2}\text{nT}$ . This justifies the experimental observation ( e.g. *Varotsos et al.* [1996a]) that small amplitude SES are not accompanied by easily observable variations of the horizontal components of the magnetic field.

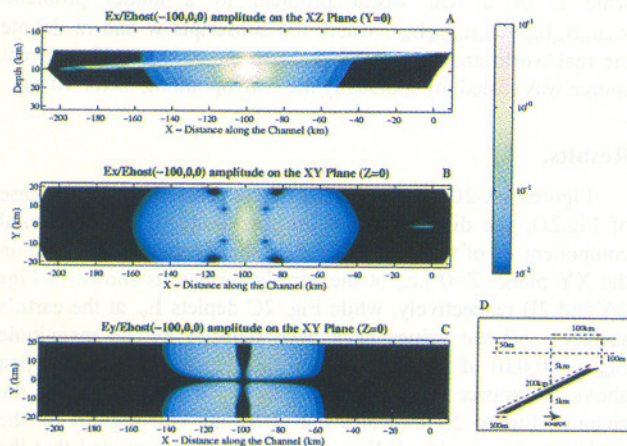


Figure 2. Calculated values of the amplitude of various components of electric field (reduced by the electric field magnitude  $E_{\text{host}}(-100,0,0)$  above the source in the absence of the channel) and the schematic diagram, not to scale, of the model used in the calculation.

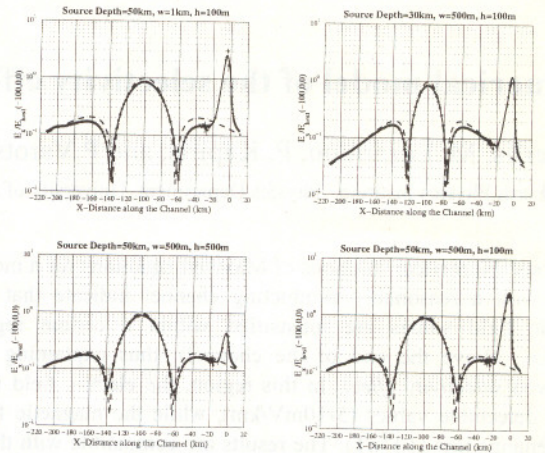


Figure 3. Calculated values of the amplitude of the horizontal component  $E_x$  of the electric field (reduced by the electric field magnitude  $E_{\text{host}}(-100,0,0)$  above the source in the absence of the channel) along the projection of the channel on the earth's surface (i.e.,  $Y=0, Z=0$ ) for various widths,  $w$ , and depths,  $D$  and  $h$ , corresponding to the model of Fig.1B. The layered earth results are also depicted with a broken line.

This does not imply that SES are not accompanied at all by magnetic field variations B, the existence of which is obligatory from Maxwell equations, but does imply that they are very small compared to those which produce (comparable) MT electric field variations and hence are not readily detectable. On the other hand, strong SES activities (e.g. related with  $M\sim 6.5$ , see *Varotsos et al.* [1996b]) were actually accompanied by detectable magnetic field variations ( $\sim 10^{-1}\text{nT}$ ). We have never "considered the absence of magnetic signal as a firm criterion to select genuine SES" as *Pham et al.* [1998,1999] claim.

**$\Delta V/L$ -criterion.**

If indeed the detectability of the SES above the upper end of the channel is due to edge effects, one may wonder whether or not the  $\Delta V/L$ -criterion (e.g., *Varotsos and Lazaridou* [1991]) still holds. Thus, we now investigate its validity in the aforementioned model of Fig. 2D. Figures 5A,B show the ratio of the  $\Delta V/L$ -values for the long and the short dipoles, "ratio

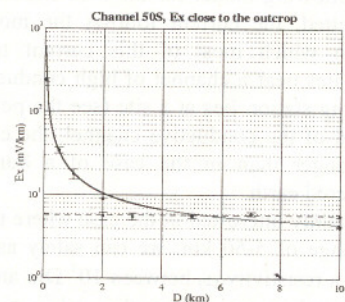
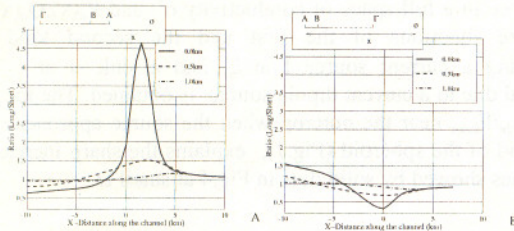


Figure 4. The electric field amplitude as measured close to the outcrop at  $(2\text{km},0,0)$  versus the distance  $D$  of the current dipole source: a) solid dots:  $D$  is the horizontal distance from the lower end of the channel as shown in Fig. 1A, b) open circles:  $D$  is the vertical distance from the channel shown in Fig. 1B. The solid line is  $3+(15/D)$  and was drawn as a guide to the eye. (Source  $100 \times 22.6\text{Am}$ , which as explained by *Varotsos et al.* [1998] might correspond to  $M\sim 5$ , if we assume solid state generation mechanisms)



**Figure 5.** The “ratio (Long/Short)”; the collinear dipoles (short: AB, long:  $A\Gamma \sim 3\text{km}$ ) are parallel to the projection of the channel on the earth’s surface, at various  $y$ -values.

(Long/Short)” hereafter, for the *asymmetric* dipole configurations discussed in *Varotsos et al.* [1996b]. In this case, a set of a long dipole and a short dipole is placed at various distances  $x$  as shown in the top part of each figure,  $x$  being measured from the projection on the earth’s surface of the channel’s upper end. The collinear dipoles were assumed to be placed parallel to the projection (which is the direction of the dominant electric field) of the channel on the earth’s surface at various  $y$ -values, i.e.,  $y=0, 0.5, \text{ and } 1.0 \text{ km}$ . These figures show the following: at short distances from the channel’s upper end, and at small  $y$ -values (e.g.,  $y \approx 0$ ), the “ratio (Long/Short)” markedly differs from unity, as expected; otherwise, this ratio remains close to unity in agreement with the SES observations.

The validity of the  $\Delta V/L$ -criterion could be also understood on the basis of the analytical solutions of the paraboloidal “edge” (*Varotsos et al.* [1998]), which not only result in strong electric fields close to the edge but also show “slow” field variation versus the distance  $\delta$  from the surface of the paraboloid i.e.,  $|E| \propto \delta^{-1+\epsilon}$ ,  $0 < \epsilon \ll 1$ . *Varotsos et al.* [1998] made use of the paraboloidal coordinates:  $x = \lambda \mu \cos(\phi)$ ,  $y = \lambda \mu \sin(\phi)$ ,  $z = 1/2(\lambda^2 - \mu^2)$ , and assumed that the conductivity in the region  $\mu < \mu_1$  bounded by the paraboloid  $\mu = \mu_1$  is  $\sigma$  and for the space outside  $\mu \geq \mu_1$  is  $\sigma'$ . The case of a point current dipole directed along the  $z$ -axis and located at  $(0, 0, z_0)$  was studied. A calculation is presented for the two conductivity ratios,  $\sigma/\sigma' = 4000/10, 1000/1$  for the case  $\mu_1 = 0.1 \sqrt{\text{km}}$  by considering a dipole source lying inside the conductive medium at a distance  $z_0 = 100 \text{ km}$  (Fig. 6). The calculation showed that in the vicinity of the vertex  $E_{\text{outside}}/E_{\text{host}} \approx \sigma/\sigma'$  (where  $E_{\text{outside}}$  and  $E_{\text{host}}$  denote the electric field values inside the resistive medium in the presence and absence of the paraboloidal edge respectively), while at distances, measured from the axis of the symmetry, around a few times the width of the conductive body (but not close to it), this ratio is of the order of  $E_{\text{outside}}/E_{\text{host}} \sim 10$  (Fig. 6C). At such distances, the enhancement of the field is still large for  $E_{\text{outside}}$  (mainly directed along the unit vector  $\mathbf{e}_\mu$ ) to be detectable, and its amplitude  $E_{\text{outside}}$  does not vary drastically, thus leading to  $\Delta V/L \approx \text{const}$ . More precisely, in Fig. 6D, the potential around the edge with respect to that at the origin in the absence of the channel is shown; the equipotential surfaces are just the equal- $\mu$  surfaces, i.e., the potential does not practically depend on  $\lambda$ , giving rise to significant  $E_{\text{outside}} \cdot \mathbf{e}_\mu$  components only.

We now investigate the dependence of the amplitude  $E_{\text{outside}}$  on the distance from the surface of the paraboloid. It should be understood that in this model, charges are accumulated on the boundary, but their distribution is not uniform. Figure 6B depicts  $E_{\text{outside}}$  versus the distance  $\delta$  (along  $\mathbf{e}_\mu$ ) from the surface of the paraboloid. At very short distances it starts with  $|E| \propto 1$ , while at larger the behaviour turns to  $|E| \propto 1/\delta$  and finally to  $|E| \propto 1/\delta^3$ ; the latter ( $1/\delta^3$ ) reminds the distance dependence of the field from a dipole, while the former ( $1/\delta$ ) reflects the non-uniform charge distribution on a sheet. The (smooth)  $1/\delta$  behaviour, which seems

to be a general behaviour of the edge effects (*Varotsos et al.* [1999a]), is dominant in the region from a few hundred meters to a few km (Fig. 6B) and provides the basis for  $\Delta V/L \approx \text{const}$ . Arranging our short and long dipoles lie along  $\mathbf{e}_\mu$  (i.e., along the direction of the dominant electric field) as shown in Fig. 6D, we obtain the contours of the “ratio (Long/Short)”, shown on Figs. 6E and 6F for the two asymmetric dipole configurations recommended by *Varotsos and Lazaridou* [1991] and *Varotsos et al.* [1993]. Figures 6E and 6F indicate that  $\Delta V/L \approx \text{const}$  (within 30%, or so) in the aforementioned extended region where  $E_{\text{outside}}/E_{\text{host}} \approx 10\text{--}20$  (Fig. 6C).

The above results show that when a conductive edge is embedded in a horizontally layered or homogeneous half-space, the  $\Delta V/L$ -values of a short dipole and a long dipole (when they are directed almost parallel to the direction  $\mathbf{e}_\mu$ , along which the electric field values may become detectable) are comparable. It is important to note that the present argument holds only for homogeneous grounds (except of the modeled channel structure) and the  $\Delta V/L$  criterion should not be applied to inhomogeneous grounds (*Varotsos and Lazaridou* [1991]). Often this simple point is disregarded such as by comparing the  $\Delta V/L$ -values of short dipoles at far apart stations [*Pham et al.*, 1998] in a strongly inhomogeneous area [*Varotsos et al.*, 1996a], or checking the equality of the  $\Delta V/L$ -values of NS dipoles at sites [*Gruszow et al.*, 1996] which have different directions of the MT electric field polarization [*Varotsos et al.*, 1996a, 1999b].

The comparison of the recordings on a set of short and long dipoles, if properly treated (*Varotsos et al.* [1999b]) and the relevant criteria published by *Varotsos and Lazaridou* [1991] are followed, is useful for the discrimination of SES from noise. *Nagao et al.* [1996] independently checked these criteria and found results essentially agreeing with those published by VAN. They emphasised that “Many of the changes are similar in appearance on the records and it is impossible to recognise SES without simultaneous recordings by multiple short dipoles in different orientations and long dipole(s)”. During the overlapping recording period (June 1997) of our group with *Pham et al.*

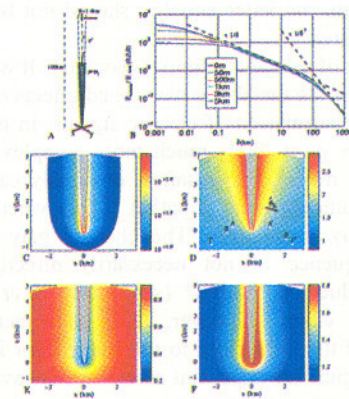


**Figure 6.** The case of a paraboloidal edge for a conductivity ratio  $\sigma/\sigma' = 1000/1$ . A) Schematic diagram of the surface  $\mu = \mu_1 = 0.1 \sqrt{\text{km}}$  separating the regions with conductivities  $\sigma$  and  $\sigma'$ . B)  $E_{\text{outside}}$  as a function of  $\delta$  (along  $\mathbf{e}_\mu$ ) measured from various points (their ordinate  $z$  are given in the inset) on its surface; the values have been reduced by the electric field value at the origin in the absence of the edge. C) The ratio  $E_{\text{outside}}/E_{\text{host}}$  on the XZ plane. D) The potential reduced by the value at the origin in the absence of the edge, along with the two short ( $\sim 100\text{m}$ ) and long ( $\sim 1\text{km}$ ) dipole configurations (not to scale) AB, A $\Gamma$  or A' $\Gamma'$ , B' $\Gamma'$ . E, F). The “ratio (Long/Short)” for the two dipole configurations AB, A $\Gamma$  or A' $\Gamma'$ , B' $\Gamma'$  as a function of the position of A or A'.

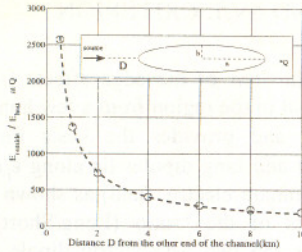


**Figure 7.** The ratio  $E_{\text{outside}}/E_{\text{host}}$  for a conductive spheroid ( $a=50\text{km}$ ,  $b=1.5\text{km}$ ) embedded in a more resistive medium (conductivity ratio  $\sigma/\sigma'=4000/10$ ). The current dipole source lies at a distance  $D$  from the one end, while the measurements are made at a point  $Q$ , 100m away from the other end. The broken line proportional to  $1/D^{0.9}$  was drawn as a guide to the eye.

[1998,1999], we could distinguish, as noise, using the aforementioned criteria, the signals they reported as SES-like.

### Concluding remarks

The present paper is based on a simple model which assumes that the dipole current source lies in the vicinity of a conductive path which terminates below the earth's surface. This model results in electric field values  $E$  that are significantly intensified (compared to the case of a homogeneous half-space or horizontally layered earth, but in the absence of the channel) in the region above the end of the channel (hereafter called AEC). Assuming that AEC lies at epicentral distances of  $d\sim 100\text{km}$ , this model can explain: First, the electric field values at AEC are larger than those measured at points on the earth's surface that may lie at shorter epicentral distances (cf. At source depths larger than a certain value, the electric field value at AEC may even become larger than that measured at the earth's surface above the source). Second, although the  $E$ -values at AEC may become detectable (5-10mV/km), the  $B$ -values are still very low, i.e., of the order of  $10^{-2}\text{nT}$ , thus not being readily detectable. Third, at AEC, the  $\Delta V/L$ -values recorded at short and long dipoles (both oriented along  $e_{\mu}$ , but not lying very close to the edge) are comparable; this has been shown when the conductive edge is embedded in a horizontally layered earth or in a homogeneous half-space. Fourth, the latter equality should not be valid in an inhomogeneous area.

The model is of extremely simple geometry. It was the aim of the model to illustrate the above mentioned effects of conducting channel on the transmission of electric signals. In the real earth, the structures are most likely much more complex. The simple geometry of our model, for instance, obviously cannot explain what the actual underground situation is like when a station is sensitive to many focal areas. The channel may consist of a complicated sequence of not necessarily directly connected (elongated) conductive "bodies" (see Varotsos et al. [1999a]). Even in such cases, however, the phenomenon of the intensification of the field close to the "edge", for instance, will still remain and play an important role. Further investigation on models closer to real earth is underway.

### Appendix: Current dipole close to a conductive spheroid

The potential inside ( $\varphi_{\text{IN}}$ ) and outside ( $\varphi_{\text{OUT}}$ ) a conducting spheroid of conductivity  $\sigma$ , embedded in a medium of conductivity  $\sigma'$  expressed in the appropriate prolate spheroidal coordinates:  $x=\alpha\cos(\phi)\sqrt{(\xi^2-1)(1-\eta^2)}/2$ ,  $y=\alpha\sin(\phi)\sqrt{(\xi^2-1)(1-\eta^2)}/2$ ,  $z=\alpha\xi\eta/2$ , for a current source  $I$  located at the principal symmetry axis of the spheroid at  $(\xi_1, -1, 0)$  outside the spheroid ( $\xi_1 > \xi_0$ ), is  $\varphi_{\text{IN}}(\xi, \eta, \phi) = I/(2\pi\alpha\sigma') \sum A_n P_n(\eta) P_n(\xi)$ , and  $\varphi_{\text{OUT}}(\xi, \eta, \phi) = I/(2\pi\alpha\sigma') \sum B_n P_n(\eta) Q_n(\xi) + \varphi^p(\xi, \eta, \phi)$ , where  $A_n = (2n+1)P_n(-1)Q_n(\xi_1)\sigma' [P_n(\xi_0)Q_n(\xi_0) - P_n(\xi_0)Q_n(\xi_0)] / [\sigma P_n(\xi_0)Q_n(\xi_0) - \sigma' P_n(\xi_0)Q_n(\xi_0)]$ ,

$B_n = (2n+1)P_n(-1)Q_n(\xi_1)(\sigma - \sigma')P_n(\xi_0)P_n(\xi_0) / [\sigma P_n(\xi_0)Q_n(\xi_0) - \sigma' P_n(\xi_0)Q_n(\xi_0)]$ ,  $\varphi^p(\xi, \eta, \phi)$  the (primary) electrostatic potential for the source in a full space of conductivity  $\sigma'$ , and  $P_n(x), Q_n(x)$  the Legendre functions of the first and the second kind. By combining a current source  $I$  at  $\xi_1$  and a sink  $-I$  at  $\xi_1'$  the potential due to a current dipole source is obtained. The increase of  $E_{\text{outside}}/E_{\text{host}}$  near the outcrop when the source approaches the other end of the spheroid (Fig.7), explains the sharp increase of the values showed by solid dots in Fig.4 at small  $D$ .

**Acknowledgements.** We express our sincere thanks to Prof. Seiya Uyeda for very useful discussions and suggestions.

### References

- Gruszow, S., J.C. Rossignol, A. Tzani, and J.L. Le Mouel, Identification and analysis of electromagnetic signals in Greece: the case of the Kozani earthquake VAN prediction, *Geophys. Res. Lett.*, 23, 2025-2029, 1996.
- Hoversten, G.M., and A. Becker, EM1DSH with EMMODEL a Motif GUI, Numerical Modeling of multiple thin 3D sheets in a layered earth, Publ. of the University of California at Berkeley, Engineering Geoscience Department, 101 pp., Berkeley, 1995.
- Nagao, T., M. Uyeshima and S. Uyeda, An independent check of VAN's criteria for signal recognition, *Geophys. Res. Lett.*, 23, 1441-1444, 1996.
- Pham, V.N., D. Boyer, G. Chouliaras, J.L. LeMouel, J.C. Rossignol, and G.N. Stavrakakis, Characteristic of electromagnetic noise in the Ioannina region (Greece); a possible origin for so called "Seismic Electric Signal" (SES), *Geophys. Res. Lett.*, 25, 2229-2232, 1998.
- Pham, V.N., D. Boyer, J.L. LeMouel, G. Chouliaras, and G.N. Stavrakakis, Electromagnetic signals generated in the solid Earth by digital transmission of radio-waves as a plausible source for some so-called "seismic electric signals", *Phys. Earth and Planet. Int.*, 114, 141-163, 1999.
- Uyeda, S., Introduction to the VAN method of earthquake prediction, in *The Critical Review of VAN: Earthquake Prediction from Seismic Electric Signals*, edited by Sir J. Lighthill, pp. 3-28, World Scientific, Singapore, 1996.
- Varotsos, P., and K. Alexopoulos, *Thermodynamics of Point Defects and their Relation with Bulk Properties*, 474 pp., North Holland, Amsterdam, 1986.
- Varotsos, P., and M. Lazaridou, Latest aspects of earthquake prediction in Greece based on Seismic Electric Signals, *Tectonophysics* 188, 321-347, 1991.
- Varotsos, P., K. Alexopoulos, and M. Lazaridou, Latest aspects of earthquake prediction in Greece based on seismic electric signals, II, *Tectonophysics* 224, 1-37, 1993.
- Varotsos P., M. Lazaridou, K. Eftaxias, G. Antonopoulos, J. Makris and J. Kopanas, Short term earthquake prediction in Greece by Seismic Electric Signals, in *The Critical Review of VAN: Earthquake Prediction from Seismic Electric Signals*, edited by Sir J. Lighthill, pp. 29-76, World Scientific, Singapore, 1996a.
- Varotsos, P., N. Sarlis, M. Lazaridou and P. Kapiris, A plausible model for the explanation of the selectivity effect of Seismic Electric Signals, *Practica of Athens Academy*, 71, 283-354, 1996b.
- Varotsos, P., N. Sarlis, M. Lazaridou, and P. Kapiris, Transmission of stress induced electric signals in dielectric media, *J. Appl. Phys.* 83, 60-70, 1998.
- Varotsos, P., N. Sarlis, and M. Lazaridou, Transmission of stress induced electric signals in dielectric media, II, (to appear in *Acta Geophysica Polonica*) 1999a.
- Varotsos, P., N. Sarlis, N. Bogris, J. Makris, P. Kapiris and A. Abdulla, A Comment on the  $\Delta V/L$ -Criterion for the Identification of the Seismic Electric Signals, in *Seismo-Atmospheric and Ionospheric Electromagnetic Phenomena*, edited by M. Hayakawa, pp. 1-45, TERRAPUB, Tokyo, 1999b.

N. Sarlis, M. Lazaridou, P. Kapiris, and P. Varotsos Solid Earth Physics Institute, University of Athens, Zografos, 15784, Athens, GREECE, (e-mail: [pvaroy@leon.nrccps.ariadne-t.gr](mailto:pvaroy@leon.nrccps.ariadne-t.gr))

(Received July 20, 1998; revised September 10, 1999; accepted September 14, 1999)